

Suppression of RGSz1 function optimizes the actions of opioid analgesics by mechanisms that involve the Wnt/ β -catenin pathway

Sevasti Gaspari^{a,b,c}, Immanuel Purushothaman^{a,b}, Valeria Cogliani^{a,b}, Farhana Sakloth^{a,b}, Rachael L. Neve^d, David Howland^e, Robert H. Ring^f, Elliott M. Ross^{g,h}, Li Shen^{a,b}, and Venetia Zachariou^{a,b,1}

^aFishberg Department of Neuroscience, Icahn School of Medicine at Mount Sinai, New York, NY 10029; ^bFriedman Brain Institute, Icahn School of Medicine at Mount Sinai, New York, NY 10029; ^cDepartment of Basic Sciences, University of Crete Medical School, 71003 Heraklion, Greece; ^dGene Delivery Technology Core, Massachusetts General Hospital, MA 02129; ^eCure Huntington's Disease Initiative (CHDI) Foundation, Princeton, NJ 08540; ^fDepartment of Psychiatry, Icahn School of Medicine at Mount Sinai, New York, NY 10029; ^gDepartment of Pharmacology, University of Texas Southwestern Medical Center, Dallas, TX 75390; and ^hGreen Center for Systems Biology, University of Texas Southwestern Medical Center, Dallas, TX 75390

Edited by Solomon H. Snyder, Johns Hopkins University School of Medicine, Baltimore, MD, and approved January 5, 2018 (received for review June 23, 2017)

Regulator of G protein signaling z1 (RGSz1), a member of the RGS family of proteins, is present in several networks expressing mu opioid receptors (MOPRs). By using genetic mouse models for global or brain region-targeted manipulations of RGSz1 expression, we demonstrated that the suppression of RGSz1 function increases the analgesic efficacy of MOPR agonists in male and female mice and delays the development of morphine tolerance while decreasing the sensitivity to rewarding and locomotor activating effects. Using biochemical assays and next-generation RNA sequencing, we identified a key role of RGSz1 in the periaqueductal gray (PAG) in morphine tolerance. Chronic morphine administration promotes RGSz1 activity in the PAG, which in turn modulates transcription mediated by the Wnt/ β -catenin signaling pathway to promote analgesic tolerance to morphine. Conversely, the suppression of RGSz1 function stabilizes Axin2-G α z complexes near the membrane and promotes β -catenin activation, thereby delaying the development of analgesic tolerance. These data show that the regulation of RGS complexes, particularly those involving RGSz1-G α z, represents a promising target for optimizing the analgesic actions of opioids without increasing the risk of dependence or addiction.

morphine | RNA sequencing | periaqueductal gray | G proteins | analgesia

Mu opioid receptor (MOPR) agonists, such as morphine, are prescribed for the treatment of severe acute or chronic pain conditions, but their long-term use is hindered by numerous side effects and by the development of dependence and addiction (1–4). Recent evidence highlights the rise of physical dependence and addiction in patients treated with opioid analgesics (5, 6). As research efforts aim to develop more efficient and safer morphine-like compounds (6, 7) and opioid alternatives, a more detailed understanding of the mechanisms mediating the analgesic effects of MOPR agonists is needed. Although information on the cellular and molecular adaptations associated with repeated exposure to opioids is emerging (8–13), the detailed brain region- and cell type-specific signal transduction events triggered by MOPR activation are not fully understood.

RGSz1, one product of the *RGS20* gene (14), is a member of the Rz subfamily [composed of GAIP (RGS19), RGSz1, RGSz2 (RGS17)] of regulator of G protein signaling (RGS) proteins (15–17) and is expressed in several brain regions (18–20). RGSz1 accelerates the hydrolysis of GTP-bound G α z more than 600-fold and may modulate the GTP hydrolysis of other G α i subunits (18, 19). As with other RGS proteins, RGSz1 may serve as an effector antagonist for G α subunits (21, 22). RGSz1 has been shown to modulate signal transduction from MOPRs and serotonin receptor 1A both in vitro (23, 24) and in vivo (25, 26) whereas knockout of the G α z subunit accelerates the development of morphine tolerance (27, 28). Although a number of studies have documented brain region-specific effects of other

RGS proteins (RGS9-2, RGS7, and RGS4) (29–33) on the functional responses of MOPRs, the role of RGSz1 in opioid actions is not known. We hypothesized that the expression and activity of RGSz1 are altered by chronic opioid use and that the manipulation of RGSz1 expression will impact the development of tolerance to the drug and its analgesic and rewarding effects.

Here, we show that chronic morphine administration increases RGSz1 expression in the periaqueductal gray (PAG), a brain region that plays a key role in modulating endogenous analgesia and responses to MOPR agonists (34). Knockout of *Rgsz1* (RGSz1KO) increased the analgesic efficacy of opioids and decreased the sensitivity to the rewarding and locomotor activating effects of morphine without impacting physical dependence. Global deletion or conditional knockdown of *Rgsz1* in the ventrolateral (vl) PAG delayed the development of morphine tolerance in pain-free and chronic pain states. Coimmunoprecipitation (co-IP) assays indicated that, under states of morphine tolerance, there is an increased formation of complexes between G α z and MOPR in the PAG. Next-generation RNA sequencing (RNA-Seq) revealed a robust down-regulation of Wnt/ β -catenin signaling in the PAG of morphine-tolerant mice. Our Co-IP and Western blot analyses also suggested that RGSz1 competes with

Significance

Opioids are used to alleviate severe pain, but their long-term use leads to analgesic tolerance, dependence, and addiction. Here, we targeted specific intracellular pathways to dissociate the analgesic actions of opioids from addiction-related effects. Using genetically modified male and female mice in models of addiction and analgesia, we revealed a key role of an intracellular modulator of the mu opioid receptor, RGSz1, in opioid actions. We applied next-generation sequencing and biochemical assays to delineate the mechanism of RGSz1 action in the mouse periaqueductal gray. Findings from this work point to novel intracellular pathways that can be targeted to optimize the actions of opioids for the treatment of chronic pain.

Author contributions: S.G., I.P., F.S., D.H., R.H.R., E.M.R., and V.Z. designed research; S.G., I.P., V.C., F.S., L.S., and V.Z. performed research; R.L.N., D.H., R.H.R., and E.M.R. contributed new reagents/analytic tools; S.G., I.P., V.C., F.S., D.H., R.H.R., L.S., and V.Z. analyzed data; and S.G., E.M.R., L.S., and V.Z. wrote the paper.

The authors declare no conflict of interest.

This article is a PNAS Direct Submission.

Published under the PNAS license.

Data deposition: The data reported in this paper have been deposited in the Gene Expression Omnibus (GEO) database, <https://www.ncbi.nlm.nih.gov/geo> (accession no. GSE109165).

¹To whom correspondence should be addressed. Email: venetia.zachariou@mssm.edu.

This article contains supporting information online at www.pnas.org/lookup/suppl/doi:10.1073/pnas.1707887115/-DCSupplemental.

Published online February 12, 2018.

Axin2 (a member of the RGS protein family and a key component of the Wnt/ β -catenin pathway that controls the nuclear translocation of β -catenin) for binding to $G\alpha_z$. Using a morphine tolerance regimen, we showed that knockout of RGSz1 stabilizes Axin2/ $G\alpha_z$ complexes, permitting the nuclear translocation of β -catenin and the transcription of target genes. Therefore, interfering with RGSz1 actions may be useful for promoting the analgesic effects of MOPR agonists while attenuating their addiction-related effects.

Results

Regulation of RGSz1 by Chronic Morphine. We initially performed Western blot analyses to test the hypothesis that repeated morphine administration regulates RGSz1 levels in brain regions associated with analgesic responses. We applied a 4-d hot plate morphine tolerance paradigm and monitored analgesic responses for 4 consecutive days in groups of mice treated with morphine (15 mg/kg). RGSz1 protein levels in the PAG were up-regulated 2 h after the last morphine injection compared with that in saline-treated controls (Fig. 1A). No RGSz1 protein was detected in PAG samples from RGSz1KO mice. This morphine treatment regimen had no effect on RGSz1 expression in the nucleus accumbens (NAc), dorsal striatum (DS), or thalamus (THAL) (Fig. S1). Notably, morphine treatment up-regulated $G\alpha_z$ levels in the PAG of both RGSz1WT and RGSz1KO mice (Fig. 1B), but levels of other $G\alpha$ subunits expressed in the PAG ($G\alpha_{i3}$, $G\alpha_o$, and $G\alpha_q$) were not altered (Fig. 1C–E). To further evaluate the association between RGSz1 and $G\alpha_z$ complexes in the PAG, we performed co-IP assays and found that morphine acutely (within 30 min) promoted the dissociation of $G\alpha_z$ from MOPRs (Fig. 1F). However, chronic morphine treatment induced the converse, promoting MOPR– $G\alpha_z$ complex formation (Fig. 1G).

However, chronic morphine treatment induced the converse, promoting MOPR– $G\alpha_z$ complex formation (Fig. 1G).

RGSz1 Knockout Enhances the Analgesic Efficacy of MOPR Agonists and Delays Morphine Tolerance. We next examined the role of RGSz1 in the analgesic actions of morphine and other MOPR agonists. In the hot plate test, male RGSz1KO mice show enhanced analgesia at lower doses of morphine compared with the responses of RGSz1WT controls (Fig. 2A). This phenotype was also observed in female RGSz1KO mice (Fig. 2A, *Inset*). The sensitivity to the analgesic effects of fentanyl and methadone was also increased in RGSz1KO mice compared with that of their RGSz1WT counterparts (Fig. 2B). We repeated the hot plate assay for 8 consecutive days to assess the impact of RGSz1 on the development of morphine analgesic tolerance. By day 3, RGSz1WT mice showed reduced responses to morphine due to the development of tolerance. Analgesic responses were significantly different between genotypes, indicating that the development of tolerance to morphine treatment (15 mg/kg, s.c.) is delayed in male (Fig. 2C) and female (Fig. 2C, *Inset*) RGSz1KO mice. We similarly assessed morphine tolerance under inflammatory pain conditions. Thermal hind paw hyperalgesia after intraplantar injection of complete Freund's adjuvant (CFA) was assessed by the Hargreaves test (35). Similar to our observations of animals in pain-free states, morphine analgesia was reduced in RGSz1WT mice after 3 d of treatment whereas it was maintained in RGSz1KO mice throughout the testing period (Fig. 2D).

Interestingly, whereas RGSz1 knockout enhanced the analgesic responses to morphine, it decreased the rewarding effects. Specifically, knockout of RGSz1 decreased the sensitivity to low morphine doses in the place preference paradigm (Fig. 3A–C).

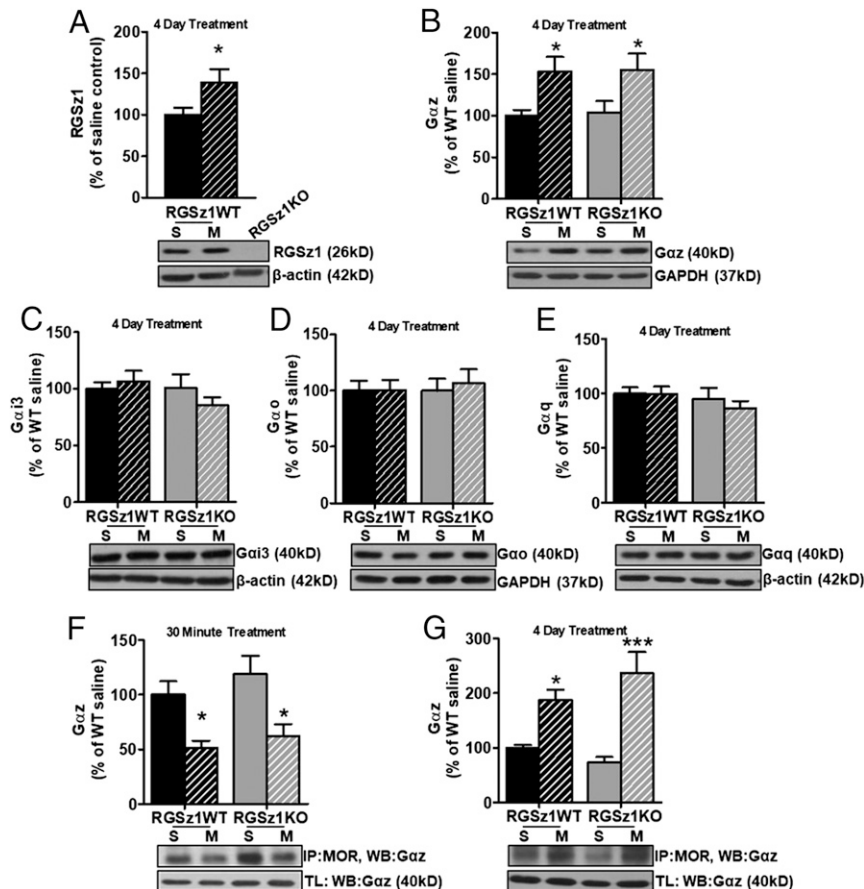


Fig. 1. Morphine regulates RGSz1 and $G\alpha_z$ in the PAG. (A) RGSz1 protein levels were elevated in the PAG of RGSz1WT mice treated for 4 consecutive days with morphine [15 mg/kg; $n = 16$ per group; t test, $t(30) = 2.144$; $*P < 0.05$]. Chronic morphine also increased the levels of $G\alpha_z$ in the PAG (B), which occurred in both RGSz1WT and RGSz1KO mice [15 mg/kg; $n = 11$ –12 per group; two-way ANOVA followed by Bonferroni's post hoc test; $F(1,42) = 11.94$; $*P < 0.05$], but not the levels of $G\alpha_{i3}$ [$F(1,42) = 0.247$] (C), $G\alpha_o$ [$F(1,42) = 0.124$] (D), or $G\alpha_q$ [$F(1,43) = 0.366$] (E) (dose: 15 mg/kg; $n = 11$ –12 per group; two-way ANOVA followed by Bonferroni's post hoc test; $F(1,12) = 17.84$; $*P < 0.05$ for all three subunits). (F) Co-IP analysis revealed that $G\alpha_z$ dissociated from MOPRs 30 min after an acute morphine injection [15 mg/kg; $n = 3$ –4 per group; two-way ANOVA followed by Bonferroni's post hoc test; $F(1,11) = 17.84$; $*P < 0.05$]. (G) However, chronic treatment with morphine for 4 consecutive days promoted MOPR– $G\alpha_z$ complexes measured 30 min after the last injection [15 mg/kg; $n = 4$ per group; two-way ANOVA followed by Bonferroni's post hoc test; $F(1,12) = 32.94$; $*P < 0.05$, $***P < 0.001$]. M, morphine; S, saline; TL, total lysate.

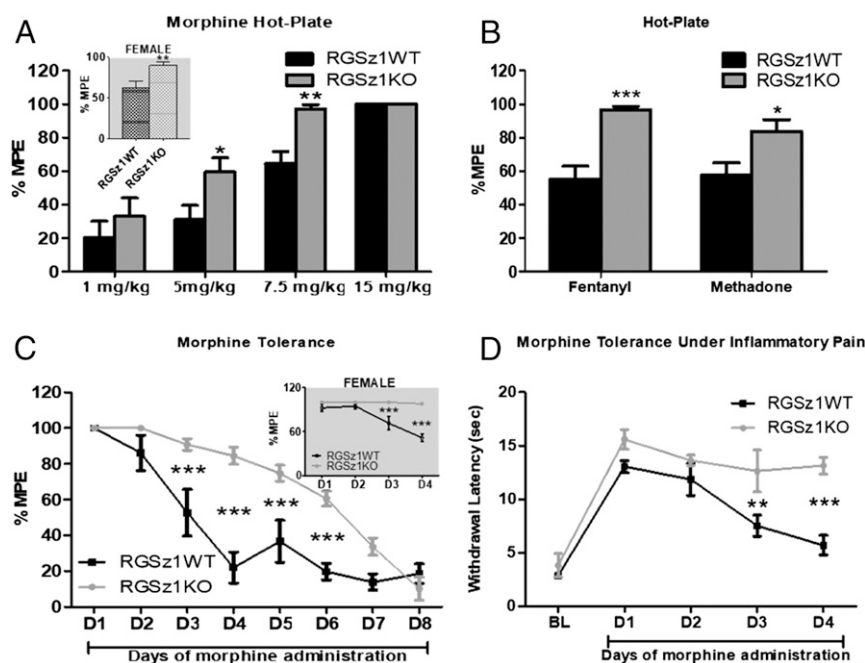


Fig. 2. Role of RGSz1 in morphine-induced analgesia. (A) Analgesic responses to morphine are enhanced in RGSz1KO mice compared with those in RGSz1WT controls [each dose was tested in a separate group of mice; $n = 8$ –10 per group; two-way ANOVA followed by Bonferroni's post hoc test, $F(1,64) = 9.28$; $*P < 0.05$, $**P < 0.01$]. A similar phenotype was observed in female mice [Inset: dose, 7.5 mg/kg; $n = 10$ –13 per group; t test, $t(21) = 2.885$; $**P < 0.001$]. (B) RGSz1KO mice show increased analgesic responses compared with those in the RGSz1WT mice to fentanyl [0.125 mg/kg; $n = 9$ –11 per genotype; t test, $t(18) = 4.677$; $***P < 0.001$] and methadone [5 mg/kg; $n = 11$ –12 per group; t test, $t(21) = 2.519$; $*P < 0.05$]. (C) The development of tolerance to 15 mg/kg morphine was delayed in male [$n = 7$ per group; two-way ANOVA repeated measures followed by Bonferroni's post hoc test, $F(1,12) = 20.99$; $***P < 0.001$] and female [Inset: $n = 6$ –7 per group; two-way ANOVA repeated measures followed by Bonferroni's post hoc test, $F(1,11) = 22.89$; $***P < 0.001$] RGSz1KO mice. (D) Delayed development of morphine tolerance was also observed under inflammatory pain states. Withdrawal latencies of hind paws with CFA-induced inflammation were significantly higher in RGSz1KO mice after 3 and 4 d, demonstrating that morphine (3 mg/kg) analgesia was maintained [$n = 4$ –5 per group; two-way ANOVA repeated measures followed by Bonferroni's post hoc test, $F(1,7) = 18.59$; $**P < 0.01$, $***P < 0.001$]. MPE, maximum possible effect.

When a higher dose of morphine was applied, both genotypes showed conditioned place preference (Fig. 3D). We also assessed locomotor activation, which is increased in rodents by repeated opioid administration (36). Knockout of *RGSz1* lowered the locomotor activation in response to repeated morphine administration (Fig. 3E). Importantly, RGSz1KO mice showed normal responses to other reward-related behaviors, such as sucrose preference [sucrose consumption (percentage of total amount consumed): RGSz1WT, 60.4 ± 6.2 ; RGSz1KO, 69.7 ± 6.2].

RGSz1 in PAG Neurons Modulates Analgesic Tolerance. We hypothesized that RGSz1 modulates the analgesic and rewarding effects of MOPR agonists via actions in distinct brain regions. To test this, we used viral approaches to conditionally knock down RGSz1 in specific brain regions of adult mice. On the basis of our initial Western blot analysis, we targeted the PAG. AAV2-CMV-CRE-GFP or an AAV2-CMV-GFP control virus was injected into the vPAG of RGSz1^{fl/fl} mice. Two weeks later, when maximal viral expression was achieved, mice were tested in the morphine tolerance paradigm. The development of morphine tolerance was significantly delayed by knockdown of RGSz1 in the vPAG (Fig. 4A), corresponding to a 50% reduction of RGSz1 protein levels (Fig. 4B). As shown in Fig. 4B and D and consistent with previous reports (37), the virus infects only neuronal cells and not astrocytes. Interestingly, the knockdown of RGSz1 in the NAc did not affect the development of analgesic tolerance (Fig. 4C). Notably, the knockdown of RGSz1 in the vPAG of male mice did not affect analgesic responses to morphine in the hot plate assay [hot plate latencies [percentage of maximal possible effect (%MPE)] for 12 mg/kg morphine: AAV2-CMV-GFP, 50.3 ± 6.7 ; AAV2-CMV-CRE-GFP, 44.2 ± 8.4].

Furthermore, the actions of RGSz1 in the vPAG did not affect the development of physical dependence. After treating mice for 5 d with escalating doses of morphine, withdrawal was precipitated with naloxone hydrochloride (1 mg/kg, s.c.). We immediately began monitoring several somatic withdrawal symptoms in AAV2-CMV-CRE-injected RGSz1^{fl/fl} mice and their AAV2-CMV-GFP-injected controls, including jumps, wet-dog shakes (WDSs), tremor, ptosis, diarrhea, and weight loss for a period of 30 min (31). As shown in Fig. 4E, withdrawal symptoms were similar between the two groups of mice. Thus, RGSz1 actions in the vPAG promote the development of analgesic tolerance without impacting the development of physical dependence.

Morphine Distinctly Alters Gene Expression Patterns in the PAG of RGSz1KO and RGSz1WT Mice. Repeated exposure to opioids promotes long-term adaptations in gene expression and neuronal plasticity (38, 39). We applied next-generation RNA-Seq to understand the impact of morphine tolerance and the influence of RGSz1 on gene expression in the PAG. PAG tissue samples were collected from mice on day 4 of the morphine hot plate assay, when analgesic tolerance emerges in RGSz1WT mice (Fig. 5A). After pooling tissue from two animals per sample, RNA from naive and morphine-treated RGSz1WT and RGSz1KO mice was analyzed. A heat map analysis comparing treated versus naive mice for each genotype showed that morphine tolerance altered gene expression patterns in RGSz1WT mice, but that a much larger number of genes were affected in the RGSz1KO group (Fig. 5B). The number of genes regulated by morphine in each genotype is shown in a Venn diagram in Fig. 5C. Our findings revealed that only one-quarter of the genes regulated by morphine were common between genotypes whereas three-quarters

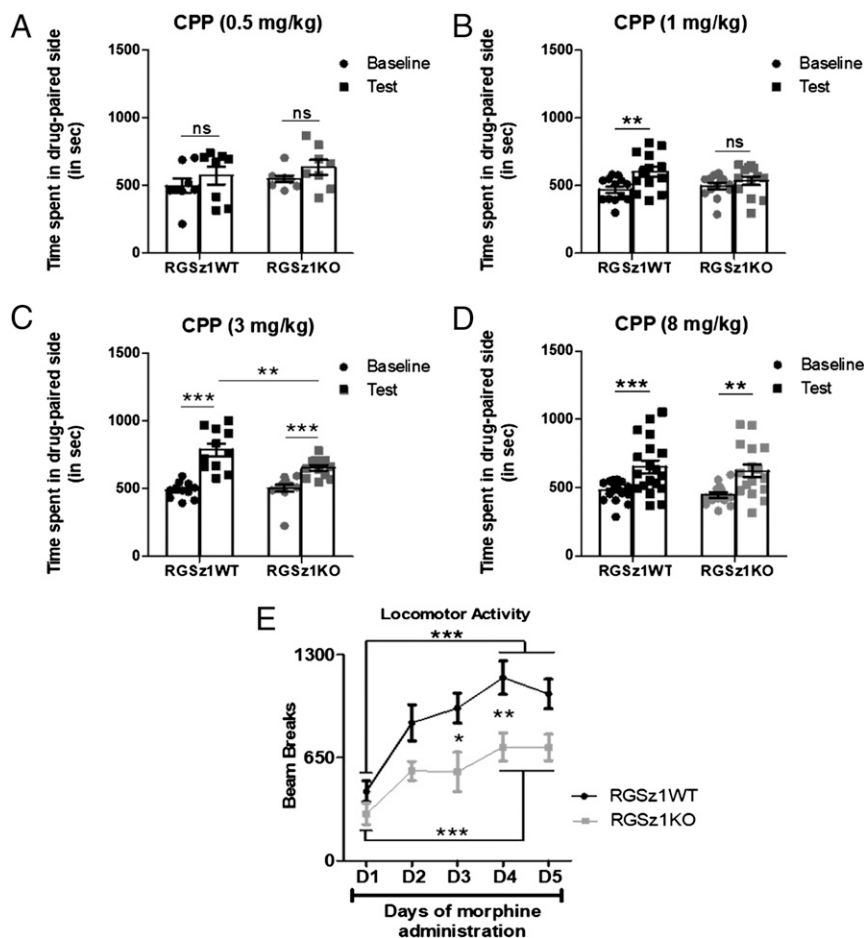


Fig. 3. RGSz1 modulates reward-like behaviors. (A–D) Knockout of RGSz1 affects the rewarding effect of low morphine doses. RGSz1KO mice did not show conditioned place preference with 1 mg/kg and spent less time in the drug-paired side when 3 mg/kg morphine was used. At higher doses (8 mg/kg), both genotypes showed conditioned place preferences to morphine [two-way repeated-measures ANOVA followed by Bonferroni's post hoc test; 0.5 mg: $n = 8$ per group, $F(1,14) = 1.12$; 1 mg: $n = 13$ per group, $F(1,24) = 0.33$, $**P < 0.01$; 3 mg: $n = 11$ –12 per group, $F(1,21) = 2.94$, $**P < 0.01$, $***P < 0.001$; 8 mg: $n = 16$ –19 per group, $F(1,33) = 0.65$, $**P < 0.01$, $***P < 0.001$]. (E) Furthermore, RGSz1KO male mice showed lower locomotor activity in response to repeated morphine administrations than RGSz1WT control mice [10 mg/kg; $n = 9$ –10 per group; two-way ANOVA repeated measures followed by Bonferroni's post hoc test, $F(1,17) = 11.16$; $*P < 0.05$, $**P < 0.01$, $***P < 0.001$]. CPP, conditioned place preference; ns, nonspecific.

of the genes with altered expression were unique to RGSz1WT or RGSz1KO mice (Fig. 5C). A gene ontology analysis indicated that the majority of genes regulated by chronic morphine in the PAG of RGSz1WT and RGSz1KO mice are associated with transcription and cell proliferation/differentiation whereas genes associated with ion/transmembrane transport, cell adhesion, and behavior are also altered in RGSz1KO mice. We further investigated this observation using ingenuity pathway analysis (IPA), and, indeed, distinct pathways in the PAG were affected in each genotype, with Wnt/ β -catenin signaling as the top pathway affected in RGSz1WT mice ($P < 0.001$) and serotonin receptor signaling targeted in RGSz1KO mice ($P < 0.001$) (Fig. 6A). Importantly, the pathway analysis of the preexisting gene expression adaptations in the PAG of RGSz1KO naive mice did not reveal alterations in any of the above-stated pathways (Fig. S3). Fig. 6B summarizes the changes in several components for each of these pathways after morphine treatment. We further validated the results by qPCR in separate cohorts of animals. Twenty selected genes per genotype were tested, and around 70% of the tested genes were validated. Differential gene expression patterns for a subset of the validated genes are presented in Fig. 6C.

Wnt/ β -Catenin Signaling Is Essential for Analgesic Responses to Morphine. Several key molecules in the Wnt/ β -catenin signaling pathway were down-regulated by chronic morphine treatment in the PAG of RGSz1WT but not RGSz1KO mice (shown in blue in Fig. 7A). Furthermore, narrowing our lists of differentially regulated genes to known β -catenin targets (40) revealed that those genes in RGSz1WT mice were primarily down-regulated (Fig. 7B). We hypothesized that analgesic responses to morphine are maintained in RGSz1KO mice because β -catenin remains

active, whereas signaling in this pathway is suppressed in RGSz1WT mice. Western blotting confirmed this hypothesis, as higher levels of active phospho- β -catenin (ser675) and inactive phospho-GSK3 β (ser9) were observed in the PAG of RGSz1KO mice after 4 d of morphine treatment (Fig. 7C and D). Furthermore, antagonism of β -catenin activity in the vPAG of RGSz1KO mice by expressing a dominant-negative form of the protein (40) induced tolerance similar to that seen in RGSz1WT controls whereas overexpressing β -catenin itself in the vPAG of RGSz1WT mice during morphine treatment was not sufficient to delay the development of tolerance (Fig. 7E; for viral validation, see Fig. S4). We therefore hypothesized that, in addition to β -catenin, other components of this pathway are necessary to obtain the prolonged analgesic response phenotype observed in RGSz1KO mice. It is also possible that the lack of an observed phenotype when β -catenin was overexpressed in the vPAG may be related to compensatory changes in the expression of destruction complex components resulting from the high levels of transgene expression. In the absence of stimulation, β -catenin is bound to Axin2 in the cytoplasm, which targets it for proteasomal degradation (41). Wnt signaling releases β -catenin for translocation to the nucleus. Because Axin2 contains an RGS domain that has been shown to interact with G α subunits (42–44), we hypothesized that an interaction between Axin2 and G α indirectly affects Wnt/ β -catenin signaling. This hypothesis was confirmed by our next set of biochemical assays. Although the total levels of Axin2 in the PAG were not affected by repeated morphine administrations (Fig. 8A), the interaction with G α in the synaptosomal fraction was significantly decreased in RGSz1WT mice, as indicated by coprecipitation of G α with

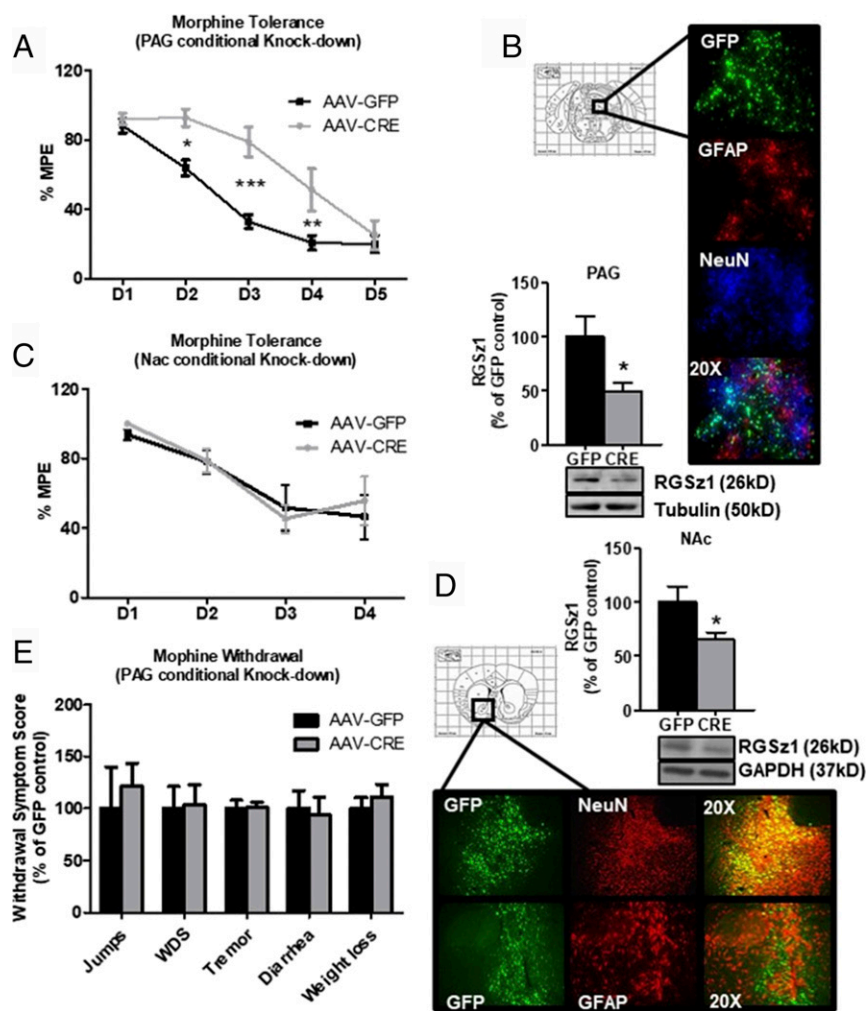


Fig. 4. *Rgsz1* knockdown in vPAG neurons suppresses morphine tolerance. (A) Conditional knockdown of *Rgsz1* in neurons in the vPAG of *Rgsz1^{fl/fl}* mice by stereotaxic infection of AAV2-CMV-CRE vectors maintained the analgesic effects of morphine in the hot plate assay over several days [15 mg/kg; $n = 7$ per group; two-way repeated-measures ANOVA followed by Bonferroni's post hoc test, $F(1,12) = 11.34$; $*P < 0.05$, $**P < 0.01$, $***P < 0.001$]. (B) Western blot analysis verifying RGSz1 down-regulation in the PAG of CRE virus-infected mice [$n = 4$ –5 per group; t test, $t(7) = 2.663$; $*P < 0.05$] and verification of AAV2 viral vector distribution in the vPAG. AAV2 vectors infect neurons (as indicated by NeuN staining) and not astrocytes (as indicated by GFAP staining). (C) The effect of *Rgsz1* knockdown on the development of morphine tolerance was region-specific, and no effect was observed when neurons of the NAc were targeted [15 mg/kg; $n = 6$ –7 per group; two-way repeated-measures ANOVA followed by Bonferroni's post hoc test, $F(1,11) = 0.08$]. (D) Western blot analysis verifying RGSz1 down-regulation in the NAc of CRE virus-infected mice [$n = 9$ –10 per group; t test, $t(7) = 2.123$; $*P < 0.05$] and verification of AAV2 viral vector distribution in the NAc. (E) Knockdown of RGSz1 in the vPAG does not affect the intensity of naloxone-precipitated morphine withdrawal symptoms ($n = 9$ –10 per group; t tests).

Axin2 (Fig. 8B). However, this interaction was maintained in RGSz1KO mice that did not exhibit morphine tolerance (Fig. 8B). The dissociation of Axin2 from Gαz was accompanied by higher levels of Axin2 in the nuclear fractions of the samples, as shown in Fig. 8C. Furthermore, a correlation analysis revealed a significant negative association between the amount of Axin2 bound to Gαz in the synaptosomal fraction and the amount of Axin2 present in the nuclear fraction (Fig. 8D). The translocation of Axin2 to the nucleus was previously shown to block β-catenin-mediated transcription (45).

Discussion

Our findings provide evidence for a brain region-specific mechanism that modulates the functional responses of MOPRs. We show that constitutive deletion of *Rgsz1* increases analgesic responses to morphine, methadone, and fentanyl and delays the development of analgesic tolerance in pain-free and chronic pain states. Importantly, the deletion of *Rgsz1* decreases the rewarding effect of morphine. These features indicate that RGSz1 is a promising target for the development of adjunct medications to enhance the efficacy of typical opioid analgesics and lower their abuse potential. Our data also indicate that the modulatory roles of RGSz1 in morphine analgesia and tolerance are the same in both male and female mice, further supporting the value of this molecule as a potential new target for pain management.

By controlling G protein-coupled receptor (GPCR) activity, RGS proteins may dynamically affect the functions of ion channels, signal transduction cascades, epigenetic modifiers, and

transcription factors (15–17, 46). Several members of the RGS family have been shown to modulate the actions of MOPR agonists in vitro and in vivo (29–33). In our previous studies, we found that RGS9-2 negatively modulates both morphine analgesia and reward-related behaviors (29, 31). Therefore, the inhibition of RGS9-2 not only improves the analgesic effects but would also likely increase the rewarding and locomotor effects of the drug and promote physical dependence. In addition, RGS9-2 has a ligand-dependent role on MOPR function, as it positively modulates the effects of fentanyl and oxycodone (30, 47). Another RGS protein, RGS7, similarly modulates both reward- and analgesia-related behaviors (32). RGS4 in the NAc has a less potent but significant effect on morphine reward, and, in the locus coeruleus, it modulates physical dependence; however, this molecule does not affect analgesia or tolerance to morphine (33). Although RGS4 and RGS7 are also expressed at moderate-to-high levels in the PAG (48), RGSz1 is unique in its differential modulation of opioid reward and analgesia.

Our study focused on understanding the mechanism by which RGSz1 modulates opioid analgesia and tolerance. Using conditional knockdown approaches, we demonstrate that the development of analgesic tolerance is fostered by RGSz1 in the vPAG, a key area involved in the descending control of pain and morphine-induced analgesia (34). Importantly, the actions of RGSz1 in the vPAG do not affect the development of physical dependence. A variety of studies document adaptations in this brain area in models of analgesic tolerance (49–52). However, the detailed mechanisms that contribute to MOPR signal

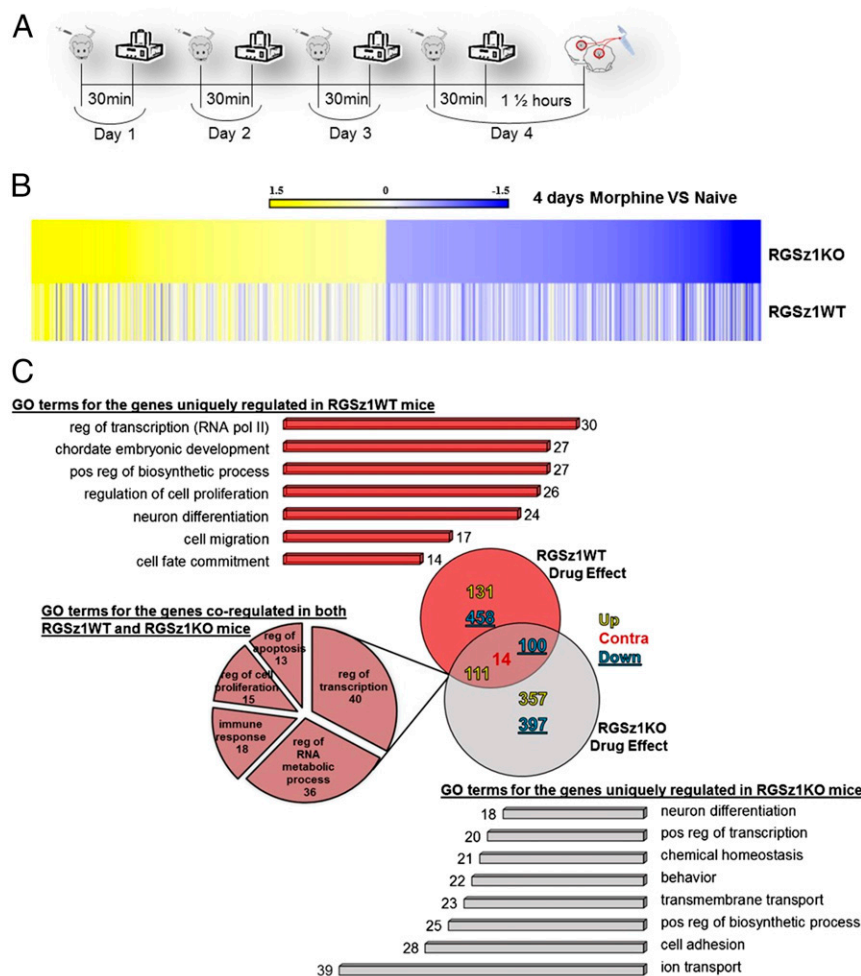


Fig. 5. RNA-Seq of PAG tissue from morphine-treated RGSz1WT and RGSz1KO mice. (A) Experimental time line showing that mice were treated for 4 consecutive days with 15 mg/kg morphine and tested in the hot plate assay to evaluate analgesic responses. On day 4 (when analgesic tolerance emerges in RGSz1WT mice), PAG tissue was collected 2 h after morphine administration. (B) Heat map analysis showing the effect of drug treatment on gene expression in RGSz1WT and RGSz1KO mice. The overall patterns of gene expression regulation were similar between the two genotypes, but a much larger group of genes were affected in the PAG of RGSz1KO mice. (C) Venn diagram depicting the actual numbers of genes affected in each group and their direction of regulation and associated Gene Ontology (GO) categories. The pie chart depicts results of a GO analysis of the 225 genes regulated by morphine in the PAG of both genotypes. Bars graphs show GO of genes uniquely regulated by morphine in the PAG of RGSz1WT (red) and RGSz1KO (light gray) mice.

transduction and desensitization in the PAG are not fully understood. Our results indicate that RGSz1 forms complexes with $G\alpha_z$ and MOPRs after chronic opioid use. These findings are in accordance with previous work by Hendry et al. (27) suggesting that compromised $G\alpha_z$ actions are associated with morphine tolerance. As mentioned above, several components of the MOPR desensitization machinery may affect the development of analgesic tolerance. This study highlighted the role of RGSz1, $G\alpha_z$, and components of the β -catenin pathway in morphine tolerance.

Our group has used next-generation sequencing in knockout mouse models and with pharmacological treatment to monitor adaptations in gene expression under pain states and to identify the pathways involved (53, 54). We applied this methodology to determine the mechanism by which chronic morphine induces analgesic tolerance and the impact of RGSz1 in such adaptations. In agreement with previously reported data, our findings indicate that analgesic tolerance to morphine is linked to robust adaptations in genes associated with inflammatory cascades (55–58), involving 8 of the 15 most significantly affected pathways identified by IPA. Notably, most of these adaptations were observed only in RGSz1WT mice and therefore are likely to be linked to morphine tolerance. Furthermore, there was a robust up-regulation of genes associated with serotonin production and release in the PAG of RGSz1KO mice, highlighting the importance of the supraspinal serotonergic system in maintaining analgesic responses (59). We observed that several components of the Wnt/ β -catenin signaling pathway were down-regulated in the RGSz1WT group at the time the mice become tolerant to morphine. Although there is no known direct link between Wnt/

β -catenin signaling and opioid actions, earlier studies have shown that the inhibition of GSK3 β , which promotes the degradation of β -catenin (41), delays the development of morphine tolerance (60, 61). Furthermore, there is evidence for Wnt/ β -catenin signaling in the morphological effects of long-term exposure to MOPR agonists, such as reduced dendritic arborization, neurite outgrowth, and neurogenesis in several brain regions (62–65). Here, we confirm the involvement of this pathway by showing that morphine tolerance can develop in RGSz1KO mice when β -catenin actions in the vPAG are directly antagonized. However, β -catenin overexpression is not sufficient to delay the development of tolerance in RGSz1WT mice, suggesting that additional factors control transcriptional activation as tolerance develops or that the robust overexpression of β -catenin affected the function of components of the destruction pathway. Our data suggest that states of morphine tolerance are associated with increased abundance of Axin2 in the nucleus, where it may repress β -catenin-mediated transcription (45).

Wnt/ β -catenin signaling is among the most conserved intracellular pathways, playing pivotal roles in cell proliferation, migration, and homeostasis (41). Therefore, the pharmacological inhibition of Wnt components would broadly affect many tissues and cellular processes in the CNS and the periphery. The identification of molecules such as RGSz1 that modulate Wnt/ β -catenin signal transduction in a brain region-specific manner may provide a novel avenue for developing adjunct medications to MOPR agonists for the management of chronic pain.

Additional research will be needed to continue to detail the actions of RGSz1 in the brain reward network and determine the

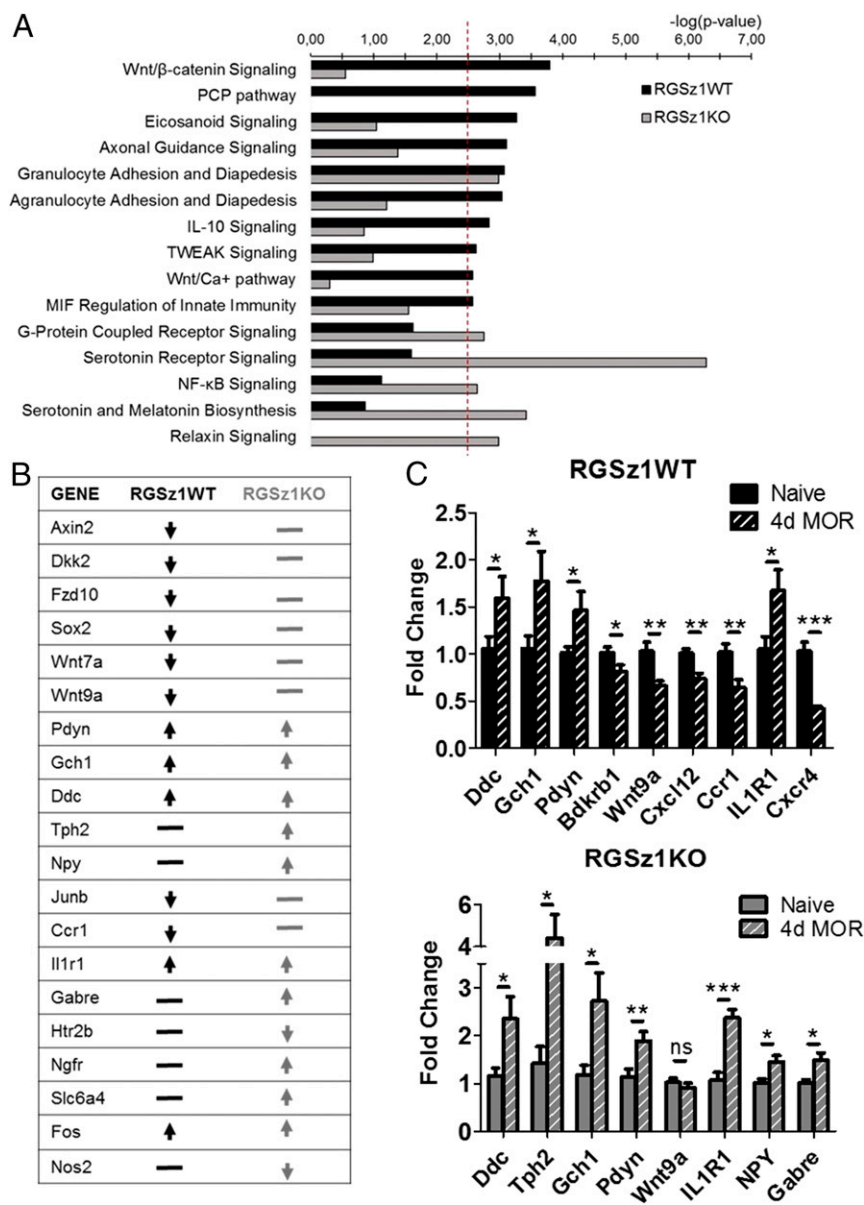


Fig. 6. Chronic morphine affects different intracellular pathways in the PAG of RGSz1KO and RGSz1WT mice. **(A)** IPA analysis of the genes regulated by chronic morphine revealed that distinct canonical pathways were affected in RGSz1WT and RGSz1KO mice (cutoff: P value < 0.003). **(B)** Selected genes in the canonical Wnt/ β -catenin signaling or inflammatory response-related cascades and G protein-coupled/serotonin receptor signaling pathways and the direction of their regulation. **(C)** qPCR validation of a subset of genes in a separate cohort of animals by genotype [$n = 7$ –8 per group; t tests, RGSz1WT: *Ddc*, $t(13) = 2.135$; *Gch1*, $t(13) = 2.2$; *Pdyn*, $t(13) = 2.27$; *Bdkrb1*, $t(14) = 2.154$; *Wnt9a*, $t(14) = 3.4$; *Cxcl12*, $t(14) = 3.69$; *Ccr1*, $t(12) = 2.99$; *Il1r1*, $t(14) = 2.44$; *Cxcr4*, $t(14) = 6.08$; RGSz1KO: *Ddc*, $t(13) = 2.29$; *Tph2*, $t(13) = 2.4$; *Gch1*, $t(13) = 2.36$; *Pdyn*, $t(13) = 2.9$; *Wnt9a*, $t(14) = 0.87$; *Il1r1*, $t(12) = 5.49$; *NPY*, $t(14) = 2.86$; *Gabre*, $t(14) = 2.98$; * $P < 0.05$, ** $P < 0.01$, *** $P < 0.001$]. ns, not significant. MIF, macrophage migration inhibitory factor; PCP, planar cell polarity; TWEAK, TNF-related adaptor molecule.

key protein interactions and intercellular pathways by which RGSz1 promotes the rewarding effects of opioids. Finally, it will be valuable to investigate if RGSz1 modulates the analgesic effects of MOPR agonists in other brain regions and the intracellular pathways involved. Overall, our findings provide information on the signal transduction networks mediating the effects of MOPR agonists in male and female mice and identify RGSz1 as a target for optimizing the analgesic actions of MOPR agonists.

Materials and Methods

Animals. For these studies, we used 2- to 3-mo-old male and female RGSz1 knockout (RGSz1KO) and WT (RGSz1WT) or RGSz1-floxed (RGSz1^{fl/fl}) mice derived from homozygote breedings. The RGSz1KO and RGSz1^{fl/fl} lines are on a DBA background, backcrossed to C57BL/6 mice for three and two generations, respectively. For the RGSz1 locus targeting strategy, see Fig. S2. The primers used for genotyping are listed in Table S1. Mice were housed with a 12-h dark/light cycle according to the Animal Care and Use Committee of the Icahn School of Medicine at Mount Sinai.

CFA Model. Chronic inflammation was induced by an intraplantar injection of 25 μ L of complete Freund's adjuvant (diluted 1:1 in saline; Sigma-Aldrich) in

the left hind paw (66). Morphine treatment (3 mg/kg) was initiated 24 h later and repeated for 4 consecutive days (day 1 to 4).

Hot Plate Analgesia Assays. Analgesia was measured using a 52 °C hot plate apparatus (IITC Life Sciences) as previously described (29). Animals were habituated in the room for 1 h, and the baseline latencies to jump or lick the hind paw were measured. Morphine was administered s.c., and, 30 min later, mice were placed on the hot plate and the latencies to jump or lick the hind paw were monitored. A cutoff time of 40 s was used to avoid tissue damage and inflammation (31). For tolerance studies, this procedure was repeated for 4 to 8 consecutive days using a high dose of morphine (15 mg/kg, s.c.). Data are expressed as percentages of maximal possible effect [MPE = (latency – baseline)/(cutoff – baseline)].

Hargreaves Assay. Morphine tolerance under inflammatory pain conditions was assessed by measuring thermal hyperalgesia in the Hargreaves test. For this assay, mice were placed in a Plexiglas box with a glass bottom, and the latency to withdraw the injured (CFA-injected) hind paw was measured after a high-intensity heat beam (30%) was applied to the midplantar area (IITC Life Sciences). Two measurements were obtained with a 10-min interval, and the average was defined as the thermal nociceptive threshold. A cutoff time of 20 s was used to avoid tissue damage (67).

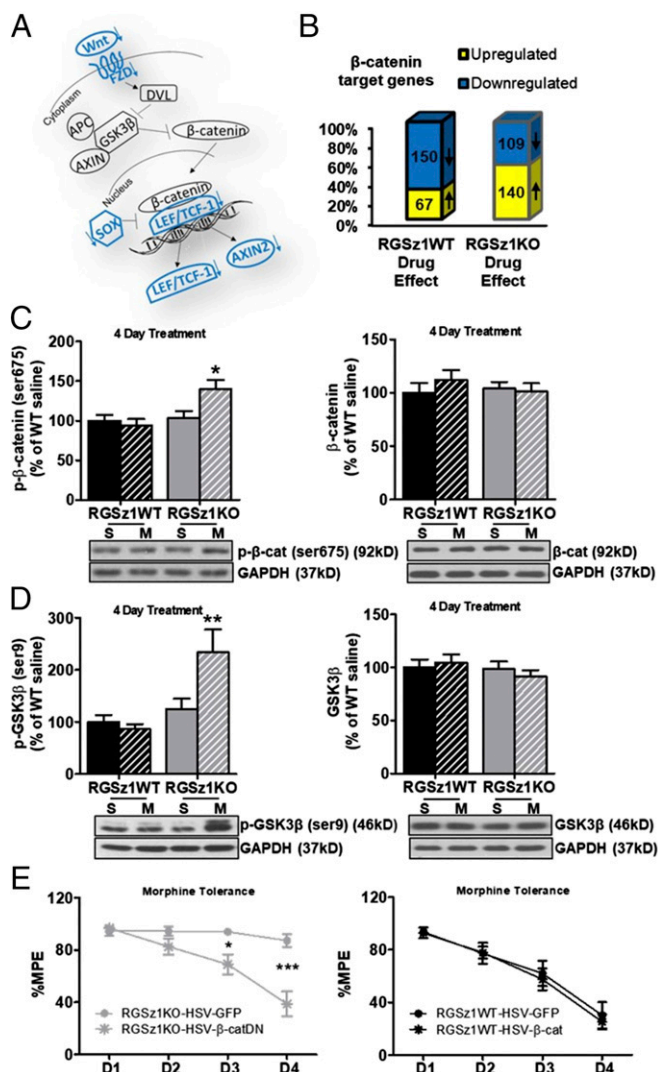


Fig. 7. RGS21 modulates the activity of the Wnt/ β -catenin signaling pathway. (A) Schematic depiction of Wnt/ β -catenin signaling pathway components (in blue) that are affected by chronic morphine in the PAG of RGS21WT mice only. (B) Bar graph showing the subset of genes that are known β -catenin targets and the direction of their regulation after chronic morphine administration. Notably, the majority of genes in the RGS21WT group were down-regulated. (C) Western blot analysis revealed regulation of active phospho- β -catenin (ser675) only in the PAG of RGS21KO mice after 4 consecutive days of morphine administration [15 mg/kg; $n = 14$ –15 per group; two-way ANOVA followed by Bonferroni's post hoc test, $F(1,53) = 7.37$; $*P < 0.05$], with total β -catenin levels remaining unaffected [$n = 11$ –12 per group; two-way ANOVA followed by Bonferroni's post hoc test, $F(1,40) = 0.18$]. (D) Levels of inactive phospho-GSK3 β (ser9) were also increased in the PAG of morphine-treated RGS21KO mice [15 mg/kg; two-way ANOVA followed by Bonferroni's post hoc test; for phospho-GSK3 β : $n = 14$ –15 per group; $F(1,53) = 11.65$, $**P < 0.01$; for total GSK3 β : $n = 11$ –12 per group; $F(1,40) = 1.004$]. (E) Antagonizing the activity of β -catenin in the vPAG by overexpressing a dominant-negative form in RGS21KO mice led to the development of analgesic tolerance to morphine [15 mg/kg; $n = 7$ for RGS21KO-HSV-GFP and 12 for RGS21KO-HSV- β -catDN; two-way repeated-measures ANOVA followed by Bonferroni's post hoc test, $F(1,51) = 9.9$; $*P < 0.05$, $***P < 0.001$]. However, overexpressing β -catenin in the vPAG of RGS21WT mice did not delay the development of analgesic tolerance [15 mg/kg; $n = 9$ for RGS21WT-HSV-GFP and 10 for RGS21WT-HSV- β -cat; two-way repeated-measures ANOVA followed by Bonferroni's post hoc test, $F(1,51) = 0.14$]. M, morphine; S, saline.

Stereotaxic Virus Injection Surgery. Conditional deletion of *Rgs21* was achieved by bilateral stereotaxic injections of the AAV2-CMV-CRE-EGFP (University of South Carolina Viral Core Facility) into the NAc or vPAG of

RGS21^{fl/fl} mice. Control animals received injections of AAV2-CMV-EGFP vectors. Stereotaxic coordinates for viral vector injections were as follows: NAc (with respect to bregma): anteroposterior (AP), +1.6 mm; anterolateral (AL), +1.5 mm; and dorsoventral (DV), –4.4 mm at 10° from the midline; vPAG (with respect to lambda): AP, +0.6 mm; mediolateral (ML), +0.8 mm; and DV, –2.8 mm at 22° from the midline. HSV- β -catenin (HSV- β -cat), HSV- β -catenin dominant negative (HSV- β -catDN), and HSV-GFP vectors were generated by R.L.N. (40).

Conditioned Place Preference Test. An unbiased place-conditioning procedure was performed using a two-chamber place-conditioning system (Med Associates, Inc.) (29, 31). Briefly, after monitoring baseline preferences for 20 min on day 1, animals were conditioned to the drug-paired or saline-paired side for 45 min on alternate days. After six conditioning sessions, animals were tested for 20 min, and the results are presented as the time spent in the drug-paired compartment at baseline compared with that on test day.

Locomotor Activation Paradigm. Mice received a saline injection (s.c.) and were habituated to the locomotor apparatus (Med Associates, Inc.) for 30 min each day for 3 consecutive days. Following that, mice received injections of morphine (10 mg/kg, s.c.) and ambulatory activity was monitored for 30 min on 5 consecutive days (47).

Opiate Withdrawal Paradigm. Mice were injected intraperitoneally (i.p.) with escalating morphine doses every 12 h for 4 consecutive days (day 1, 20 mg/kg; day 2, 40 mg/kg; day 3, 60 mg/kg; day 4, 80 mg/kg). On the 5th day, they were injected with 80 mg/kg morphine in the morning, and withdrawal was precipitated 3 h later using naloxone hydrochloride (1 mg/kg, s.c.; Sigma) (31). Withdrawal signs (jumps, wet-dog shakes, tremor, diarrhea, and weight loss) were monitored for 30 min after naloxone administration. Data are expressed as the percentages of the AAV2-GFP-injected control. For tremor and ptosis, we monitored the presence of signs at the beginning of each 5-min interval during the monitoring period (29).

Western Blotting, Subcellular Fractionations, and Co-IP Assays. Two 14-gauge PAG punches (derived from a single animal) were used per sample for all assays. Western blotting was performed as previously described (53). For subcellular fractionation, samples were homogenized using a pestle in 50 μ L of hypotonic cell lysis buffer (HCLB) plus protease and phosphatase inhibitors, incubated on ice for 45 min, and centrifuged at 371 \times g at 4 °C for 10 min, and supernatants were collected as the crude cytoplasmic fractions. The remaining nuclear pellets were washed twice with 100 μ L of HCLB plus inhibitors, resuspended in 25 μ L of nuclear lysis buffer with inhibitors, incubated for 2 h on ice, and centrifuged at 16,363 \times g at 4 °C for 5 min, and the supernatants were collected as the crude nuclear fractions. To obtain the synaptosomal fractions, the crude cytoplasmic fractions were centrifuged twice to remove the remaining nuclei (371 \times g at 4 °C for 10 min). The supernatants were collected and centrifuged at 9,361 \times g at 4 °C for 10 min. Supernatants were collected as the cytoplasmic fractions, and the synaptosomal pellets were resuspended in 20 μ L of HCLB.

Co-IPs for MOPR-Guz were performed using whole lysate samples as previously reported (30). For co-IPs with Axin2, 1 μ L of antibody was added to each synaptosomal fraction (co-IP with anti-GFP was used as the negative control), and samples were incubated overnight at 4 °C on a circular rotator. Each sample was then incubated for an additional 3 h with 10 μ L of anti-rabbit Dynabeads (Thermo Fisher Scientific). Co-IP proteins were washed three times with 700 μ L of blocking solution using a magnetic stand and then resuspended in 10 μ L of radioimmunoprecipitation assay (RIPA) buffer. The following rabbit antibodies were used: anti-RGS21 (19), anti-Guz (no. 3904; Cell Signaling), anti-G α i3 (Lilly Jiang, University of Texas Southwestern Medical Center, Dallas, TX) (68), anti-G α o (no. 3975; Cell Signaling), anti-G α q (Paul Sternweis, University of Texas Southwestern Medical Center, Dallas, TX) (69), anti-MOPR (no. 24216; Immunostar), anti-phospho- β -catenin (ser675, no. 4176; Cell Signaling), anti- β -catenin (no. 9562; Cell Signaling), anti-phospho-GSK3 β (ser9 no. 9336; Cell Signaling), anti-GSK3 β (no. 9315; Cell Signaling), anti-Axin2 (no. ab32197; Abcam), anti-GADPH (no. 5174; Cell Signaling), anti- β -actin (no. 4967; Cell Signaling), and anti-GFP (no. ab290; Abcam). Mouse anti- β -tubulin III (no. T8578; Sigma), GADPH, or β -actin antibodies were used as the loading control. Data are calculated as the optical density ratio of sample/loading control or IP/total lysate in the case of co-IPs and are expressed as the percentages of the control group. Bands were quantified using Image J software (53).

RNA-Seq and qPCR. Four biological replicates per group were used for the RNA-Seq studies. PAG punches from two animals were pooled per biological

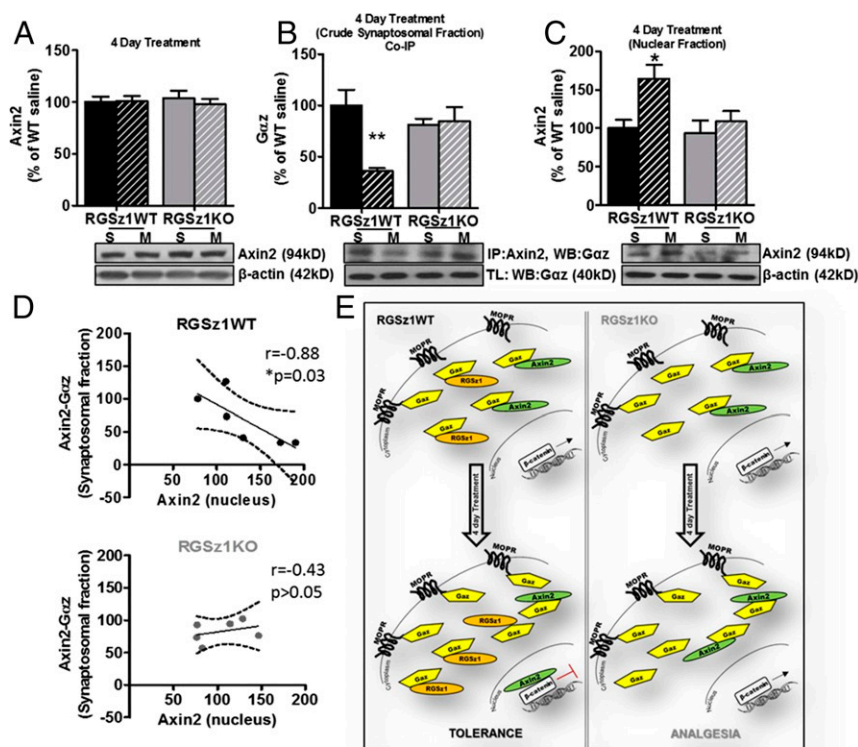


Fig. 8. RGSz1 knockout prevents dissociation of Axin2-G α z complexes after chronic morphine. (A) Protein levels of Axin2 in the PAG were not affected by morphine treatment in RGSz1WT or RGSz1KO mice [15 mg/kg; $n = 12$ per group; two-way ANOVA followed by Bonferroni's post hoc test, $F(1,44) = 0.19$]. (B) Co-IP assays on synaptosomal fractions revealed a reduced association of Axin2 with G α z in RGSz1WT but not in RGSz1KO mice after repeated morphine administration [15 mg/kg; $n = 3$ per group; two-way ANOVA followed by Bonferroni's post hoc test; $F(1,8) = 7.6$; $**P < 0.01$]. (C) Morphine tolerance in RGSz1WT also led to higher levels of Axin2 in the nucleus [15 mg/kg; $n = 3$ per group; two-way ANOVA followed by Bonferroni's post hoc test; $F(1,8) = 7$; $*P < 0.05$]. (D) Correlation analysis revealed a negative association between the amount of Axin2 bound to G α z in the synaptosomal fractions and the amount of Axin2 in the nuclear fractions of the same samples from RGSz1WT but not RGSz1KO mice. (E) Schematic depicting working hypothesis. In the PAG of tolerant mice, higher levels of RGSz1 and stabilized complexes between MOPR and G α z lead to a reduced Axin2-G α z interaction, thereby enabling the function of Axin2-containing destruction complexes, as well as the translocation of Axin2 to the nucleus and silencing β -catenin-mediated transcription. In the absence of RGSz1, Axin2 is maintained in the cytoplasm and forms complexes with G α z whereas β -catenin may translocate to the nucleus to promote transcriptional activity. M, morphine; S, saline; TL, total lysate.

replicate (four 14-gauge punches per sample). Total RNA was isolated with TRIzol, and the integrity was confirmed with an Agilent 2100 Bioanalyzer (53). mRNA-Seq libraries were prepared using a TruSeq RNA sample preparation kit v2 (Illumina). Sequencing was performed using the Illumina HiSeq 2000 apparatus. Read alignment, read counting, and differential analysis were performed using TopHat2 (70), HTSeq (71), and voom-limma R package (72), respectively. For all four gene lists, a cutoff of P value of <0.05 and $\log_2(\text{fold change})$ of <-0.5 or >0.5 were used to generate gene lists for further bioinformatics analysis. qPCR was performed using SYBR green and analyzed using the $\Delta\Delta C_T$ method. Information on primers used for biological validations is provided in Table S1.

Bioinformatics Analysis. Heat maps were generated using GENE-E. Venn diagrams were generated using VennPlex Version 1.0.0.2 (NIH), pathway analysis was conducted using IPA, and Gene Ontology (GO) analysis was conducted using the Database for Annotation, Visualization and Integrated Discovery (DAVID). For pathway analysis, a cutoff of P value of <0.003 was applied to the output pathways.

- Dart RC, et al. (2015) Trends in opioid analgesic abuse and mortality in the United States. *N Engl J Med* 372:241–248.
- Ray WA, Chung CP, Murray KT, Hall K, Stein CM (2016) Prescription of long-acting opioids and mortality in patients with chronic noncancer pain. *JAMA* 315:2415–2423.
- Ling W, Mooney L, Hillhouse M (2011) Prescription opioid abuse, pain and addiction: Clinical issues and implications. *Drug Alcohol Rev* 30:300–305.
- Walwyn WM, Miotto KA, Evans CJ (2010) Opioid pharmaceuticals and addiction: The issues, and research directions seeking solutions. *Drug Alcohol Depend* 108:156–165.
- Walter C, Knothe C, Löscher J (2016) Abuse-deterrent opioid formulations: Pharmacokinetic and pharmacodynamic considerations. *Clin Pharmacokinet* 55:751–767.

Statistical Analysis. For the experiments monitoring behavior of the same group of mice over time (Figs. 2 C and D, 3, 4 A and C, and 7 E and Fig. S2B), we used two-way repeated-measures ANOVAs followed by Bonferroni's post hoc tests. For two-factor designs (Figs. 1 B–G, 2A, and 7 C and D and Fig. S2C), we used two-way ANOVAs followed by Bonferroni's post hoc tests. For data containing a single independent variable (Figs. 1A, Upper, 2A, and 4B and Fig. S2 D and E), we used unpaired two-tailed t tests. For the data in graphs depicting multiple individual single-factor comparisons (Figs. 2B, 4E, and 6C), we used multiple t tests. Correlation analysis (Fig. 8D) was conducted using Spearman's rho. Error bars are depicting \pm SEM. F and t values for each dataset are provided in the figure legends.

ACKNOWLEDGMENTS. This work was supported by National Institute on Drug Abuse Grant PPG-POIDA08227 (to V.Z.), National Institute of Neurological Disorders and Stroke (NINDS) Grant NS086444 (to V.Z.), NINDS Grant NS093537 (to V.Z.), National Institute of General Medical Sciences Grant R01030355 (to E.M.R.), and National Institute of Deafness and Other Communication Disorders (NIDCD) Grant R21DC015744 (to E.M.R.).

- Skolnick P, Volkow ND (2016) Re-energizing the development of pain therapeutics in light of the opioid epidemic. *Neuron* 92:294–297.
- Manglik A, et al. (2016) Structure-based discovery of opioid analgesics with reduced side effects. *Nature* 537:185–190.
- Cahill CM, Walwyn W, Taylor AMW, Pradhan AAA, Evans CJ (2016) Allostatic mechanisms of opioid tolerance beyond desensitization and downregulation. *Trends Pharmacol Sci* 37:963–976.
- Kreek MJ, et al. (2012) Opiate addiction and cocaine addiction: Underlying molecular neurobiology and genetics. *J Clin Invest* 122:3387–3393.
- Contet C, Kieffer BL, Befort K (2004) Mu opioid receptor: A gateway to drug addiction. *Curr Opin Neurobiol* 14:370–378.

11. Bailey CP, Connor M (2005) Opioids: Cellular mechanisms of tolerance and physical dependence. *Curr Opin Pharmacol* 5:60–68.
12. Trang T, et al. (2015) Pain and poppies: The good, the bad, and the ugly of opioid analgesics. *J Neurosci* 35:13879–13888.
13. Raeahel KM, Bohn LM (2014) β -arrestins: Regulatory role and therapeutic potential in opioid and cannabinoid receptor-mediated analgesia. *Handb Exp Pharmacol* 219:427–443.
14. Barker SA, Wang J, Sierra DA, Ross EM (2001) RGS21 and Ret RGS: Two of several splice variants from the gene RGS20. *Genomics* 78:223–229.
15. Gerber KJ, Squires KE, Hepler JR (2016) Roles for regulator of G protein signaling proteins in synaptic signaling and plasticity. *Mol Pharmacol* 89:273–286.
16. Sjögren B, Blazer LL, Neubig RR (2010) Regulators of G protein signaling proteins as targets for drug discovery. *Prog Mol Biol Transl Sci* 91:81–119.
17. Kimple AJ, Bosch DE, Giguère PM, Siderovski DP (2011) Regulators of G-protein signaling and their G α substrates: Promises and challenges in their use as drug discovery targets. *Pharmacol Rev* 63:728–749.
18. Glick JL, Meigs TE, Miron A, Casey PJ (1998) RGSZ1, a Gz-selective regulator of G protein signaling whose action is sensitive to the phosphorylation state of G α 12. *J Biol Chem* 273:26008–26013.
19. Wang J, et al. (1998) RGSZ1, a Gz-selective RGS protein in brain. Structure, membrane association, regulation by Galphax phosphorylation, and relationship to a Gz gtpase-activating protein subfamily. *J Biol Chem* 273:26014–26025.
20. Larmine C, et al. (2004) Selective expression of regulators of G-protein signaling (RGS) in the human central nervous system. *Brain Res Mol Brain Res* 122:24–34.
21. Hepler JR, Berman DM, Gilman AG, Kozasa T (1997) RGS4 and GAIP are GTPase-activating proteins for Gq alpha and block activation of phospholipase C beta by gamma-thio-GTP-Gq alpha. *Proc Natl Acad Sci USA* 94:428–432.
22. Anger T, Zhang W, Mende U (2004) Differential contribution of GTPase activation and effector antagonism to the inhibitory effect of RGS proteins on Gq-mediated signaling in vivo. *J Biol Chem* 279:3906–3915.
23. Ajit SK, et al. (2007) RGSZ1 interacts with protein kinase C interacting protein PKC1-1 and modulates mu opioid receptor signaling. *Cell Signal* 19:723–730.
24. Ghavami A, et al. (2004) Differential effects of regulator of G protein signaling (RGS) proteins on serotonin 5-HT1A, 5-HT2A, and dopamine D2 receptor-mediated signaling and adenylyl cyclase activity. *Cell Signal* 16:711–721.
25. Creech RD, Li Q, Carrasco GA, Van de Kar LD, Muma NA (2012) Estradiol induces partial desensitization of serotonin 1A receptor signaling in the paraventricular nucleus of the hypothalamus and alters expression and interaction of RGSZ1 and G α z. *Neuropharmacology* 62:2040–2049.
26. Garzón J, Rodríguez-Muñoz M, López-Fando A, García-España A, Sánchez-Blázquez P (2004) RGSZ1 and GAIP regulate mu- but not delta-opioid receptors in mouse CNS: Role in tachyphylaxis and acute tolerance. *Neuropsychopharmacology* 29:1091–1104.
27. Hendry IA, et al. (2000) Hypertolerance to morphine in Gz (alpha)-deficient mice. *Brain Res* 870:10–19.
28. Yang J, et al. (2000) Loss of signaling through the G protein, Gz, results in abnormal platelet activation and altered responses to psychoactive drugs. *Proc Natl Acad Sci USA* 97:9984–9989.
29. Gaspari S, et al. (2014) Nucleus accumbens-specific interventions in RGS9-2 activity modulate responses to morphine. *Neuropsychopharmacology* 39:1968–1977.
30. Psifogeorgou K, et al. (2011) A unique role of RGS9-2 in the striatum as a positive or negative regulator of opiate analgesia. *J Neurosci* 31:5617–5624, and erratum (2011) 31:7578.
31. Zachariou V, et al. (2003) Essential role for RGS9 in opiate action. *Proc Natl Acad Sci USA* 100:13656–13661.
32. Sutton LP, et al. (2016) Regulator of G-protein signaling 7 regulates reward behavior by controlling opioid signaling in the striatum. *Biol Psychiatry* 80:235–245.
33. Han M-H, et al. (2010) Brain region specific actions of regulator of G protein signaling 4 oppose morphine reward and dependence but promote analgesia. *Biol Psychiatry* 67:761–769.
34. Reichling DB, Kwiat GC, Basbaum AI (1988) Anatomy, physiology and pharmacology of the periaqueductal gray contribution to antinociceptive controls. *Prog Brain Res* 77:31–46.
35. Hargreaves K, Dubner R, Brown F, Flores C, Joris J (1988) A new and sensitive method for measuring thermal nociception in cutaneous hyperalgesia. *Pain* 32:77–88.
36. Robinson TE, Berridge KC (1993) The neural basis of drug craving: An incentive-sensitization theory of addiction. *Brain Res Brain Res Rev* 18:247–291.
37. Taymans J-M, et al. (2007) Comparative analysis of adeno-associated viral vector serotypes 1, 2, 5, 7, and 8 in mouse brain. *Hum Gene Ther* 18:195–206.
38. Robison AJ, Nestler EJ (2011) Transcriptional and epigenetic mechanisms of addiction. *Nat Rev Neurosci* 12:623–637.
39. Russo SJ, et al. (2010) The addicted synapse: Mechanisms of synaptic and structural plasticity in nucleus accumbens. *Trends Neurosci* 33:267–276.
40. Dias C, et al. (2014) β -catenin mediates stress resilience through Dicer1/microRNA regulation. *Nature* 516:51–55.
41. Clevers H (2006) Wnt/ β -catenin signaling in development and disease. *Cell* 127:469–480.
42. Egger-Adam D, Katanaev VL (2010) The trimeric G protein Go inflicts a double impact on axin in the Wnt/frizzled signaling pathway. *Dev Dyn* 239:168–183.
43. Stemmler LN, Fields TA, Casey PJ (2006) The regulator of G protein signaling domain of axin selectively interacts with Galpha12 but not Galpha13. *Mol Pharmacol* 70:1461–1468.
44. Castellone MD, Teramoto H, Williams BO, Druey KM, Gutkind JS (2005) Prostaglandin E2 promotes colon cancer cell growth through a Gs-axin-beta-catenin signaling axis. *Science* 310:1504–1510.
45. Rennoll SA, Konsavage WM, Jr, Yochum GS (2014) Nuclear AXIN2 represses MYC gene expression. *Biochem Biophys Res Commun* 443:217–222.
46. Terzi D, Stergiou E, King SL, Zachariou V (2009) Regulators of G protein signaling in neuropsychiatric disorders. *Prog Mol Biol Transl Sci* 86:299–333.
47. Gaspari S, et al. (2017) RGS9-2 modulates responses to oxycodone in pain-free and chronic pain states. *Neuropsychopharmacology* 42:1548–1556.
48. Gold SJ, Ni YG, Dohlman HG, Nestler EJ (1997) Regulators of G-protein signaling (RGS) proteins: Region-specific expression of nine subtypes in rat brain. *J Neurosci* 17:8024–8037.
49. Macey TA, et al. (2009) Extracellular signal-regulated kinase 1/2 activation counteracts morphine tolerance in the periaqueductal gray of the rat. *J Pharmacol Exp Ther* 331:412–418.
50. Lane DA, Patel PA, Morgan MM (2005) Evidence for an intrinsic mechanism of antinociceptive tolerance within the ventrolateral periaqueductal gray of rats. *Neuroscience* 135:227–234.
51. Bagley EE, Chieng BCH, Christie MJ, Connor M (2005) Opioid tolerance in periaqueductal gray neurons isolated from mice chronically treated with morphine. *Br J Pharmacol* 146:68–76.
52. Bobeck EN, Chen Q, Morgan MM, Ingram SL (2014) Contribution of adenylyl cyclase modulation of pre- and postsynaptic GABA neurotransmission to morphine antinociception and tolerance. *Neuropsychopharmacology* 39:2142–2152.
53. Mitsi V, et al. (2015) RGS9-2—Controlled adaptations in the striatum determine the onset of action and efficacy of antidepressants in neuropathic pain states. *Proc Natl Acad Sci USA* 112:E5088–E5097.
54. Descalzi G, et al. (2017) Neuropathic pain promotes adaptive changes in gene expression in brain networks involved in stress and depression. *Sci Signal* 10:eaaj1549.
55. Hutchinson MR, et al. (2011) Exploring the neuroimmunopharmacology of opioids: An integrative review of mechanisms of central immune signaling and their implications for opioid analgesia. *Pharmacol Rev* 63:772–810.
56. Johnston IN, et al. (2004) A role for proinflammatory cytokines and fractalkine in analgesia, tolerance, and subsequent pain facilitation induced by chronic intrathecal morphine. *J Neurosci* 24:7353–7365.
57. Watkins LR, et al. (2007) Norman Cousins Lecture. Glia as the “bad guys”: Implications for improving clinical pain control and the clinical utility of opioids. *Brain Behav Immun* 21:131–146.
58. Mélik Parsadaniantz S, Rivat C, Rostène W, Réaux-Le Goazigo A (2015) Opioid and chemokine receptor crosstalk: A promising target for pain therapy? *Nat Rev Neurosci* 16:69–78.
59. Tao R, Ma Z, Auerbach SB (1998) Alteration in regulation of serotonin release in rat dorsal raphe nucleus after prolonged exposure to morphine. *J Pharmacol Exp Ther* 286:481–488.
60. Parkitna JR, et al. (2006) Effects of glycogen synthase kinase 3beta and cyclin-dependent kinase 5 inhibitors on morphine-induced analgesia and tolerance in rats. *J Pharmacol Exp Ther* 319:832–839.
61. Liao W-W, et al. (2014) Coadministration of glycogen-synthase kinase 3 inhibitor with morphine attenuates chronic morphine-induced analgesic tolerance and withdrawal syndrome. *J Chin Med Assoc* 77:31–37.
62. Jin J, et al. (2010) Interaction of the mu-opioid receptor with GPR177 (Wntless) inhibits Wnt secretion: Potential implications for opioid dependence. *BMC Neurosci* 11:33.
63. Reyes BA, et al. (2012) Opiate agonist-induced re-distribution of Wntless, a mu-opioid receptor interacting protein, in rat striatal neurons. *Exp Neurol* 233:205–213.
64. Li Y, Wang H, Niu L, Zhou Y (2007) Chronic morphine exposure alters the dendritic morphology of pyramidal neurons in visual cortex of rats. *Neurosci Lett* 418:227–231.
65. Eisch AJ, Barrot M, Schad CA, Self DW, Nestler EJ (2000) Opiates inhibit neurogenesis in the adult rat hippocampus. *Proc Natl Acad Sci USA* 97:7579–7584.
66. Latremoliere A, et al. (2015) Reduction of neuropathic and inflammatory pain through inhibition of the tetrahydrobiopterin pathway. *Neuron* 86:1393–1406.
67. Terzi D, et al. (2014) RGS9-2 modulates sensory and mood related symptoms of neuropathic pain. *Neurobiol Learn Mem* 115:43–48.
68. Mumby SM, Gilman AG (1991) Synthetic peptide antisera with determined specificity for G protein alpha or beta subunits. *Methods Enzymol* 195:215–233.
69. Gutowski S, et al. (1991) Antibodies to the alpha q subfamily of guanine nucleotide-binding regulatory protein alpha subunits attenuate activation of phosphatidylinositol 4,5-bisphosphate hydrolysis by hormones. *J Biol Chem* 266:20519–20524.
70. Kim D, et al. (2013) TopHat2: Accurate alignment of transcriptomes in the presence of insertions, deletions and gene fusions. *Genome Biol* 14:R36.
71. Anders S, Pyl PT, Huber W (2015) HTSeq—A Python framework to work with high-throughput sequencing data. *Bioinformatics* 31:166–169.
72. Law CW, Chen Y, Shi W, Smyth GK (2014) voom: Precision weights unlock linear model analysis tools for RNA-seq read counts. *Genome Biol* 15:R29.